

Unusual plasmon dispersion in the quasi-one-dimensional conductor $(\text{TaSe}_4)_2\text{I}$: Experiment and theory

M. Sing, V. G. Grigoryan, G. Paasch, M. Knupfer, and J. Fink
Institut für Festkörper- und Werkstofforschung Dresden, D-01171 Dresden, Germany

H. Berger and F. Lévy
Laboratoire de Physique Appliquée, Ecole Polytechnique Fédérale, CH-1015 Lausanne, Switzerland

(Received 30 January 1998)

We present a combined experimental and theoretical study of the plasmon dispersion in a quasi-one-dimensional conductor, the transition metal tetrachalco-halogenide $(\text{TaSe}_4)_2\text{I}$. The dispersion relation, as measured by electron energy-loss spectroscopy in transmission, is quasilinear, which is not expected from the literature. However, we show that the data can be explained within a one-band model, which additionally allows the derivation of the conduction-band dispersion. Thus, contrary to evidence from photoemission measurements, we find no hint for singular properties caused by one dimensionality. [S0163-1829(98)07419-0]

I. INTRODUCTION

Renewed, ongoing interest in the peculiar phenomena regarding the physics of one-dimensional electron systems has been evoked by recent high-resolution photoemission measurements of quasi-one-dimensional (Q1D) compounds such as $\text{K}_{0.3}\text{MoO}_3$ or $(\text{TaSe}_4)_2\text{I}$.¹⁻³ Although these materials are Peierls systems with a metal-insulator transition at 183 (Ref. 4) and 263 K,⁵ respectively, no characteristic Fermi step could be seen in the metallic phase, as is expected and observed in the case of two- or three-dimensional systems. This observation was attributed to the well-known instability of the Fermi-liquid (FL) ground state of a system of electrons confined to one dimension as the Coulomb interaction between them is switched on. Nevertheless, an attempt to explain the experimental data within the picture of a Luttinger liquid (LL) (Ref. 6) led to an unphysically high value for the exponent describing the power-law behavior of the spectral function in the vicinity of the Fermi energy.^{7,8} Recently, a possible justification for such a high value has been offered by demonstrating that the inclusion of the interchain interaction mediated by the Coulomb forces, which is always present in real systems, can lead to larger values for this exponent.⁹ This also remains true for a nonzero but sufficiently small electron hopping probability between the chains although, strictly speaking, one is then no longer dealing with a LL but with a FL. It has been argued that this crossover between a LL and a FL due to electron hopping (in the presence of the interchain interaction) should be irrelevant in an intermediate regime of momenta and frequencies in experiments such as photoemission spectroscopy (PES), for example.⁹ However, other possible causes,¹⁻³ which were discussed for this suppression or redistribution of spectral weight reaching down about 0.5 eV below the Fermi energy, such as large fluctuation effects, strong electron-phonon interactions, a real lack of states at the Fermi energy, or surface degradation, cannot be ruled out completely. On the other hand, a thorough experimental and theoretical study of the dc conductivity and the temperature dependence of the Peierls gap below and the pseudogap above the transition tempera-

ture showed that an adequate understanding of the dc electrical transport can be achieved based on a quasiclassical formulation in terms of the Boltzmann equation. This approach requires only minimal information about the band structure and includes just the temperature-dependent gap as a specific 1D feature.^{10,11} Starting from the conjecture that the photoemission data do provide some evidence for a singular 1D phenomenology (whereas it is clear that the dc transport properties do not), our approach to shedding light on this question is the careful investigation of the bulk plasmon dispersion along the 1D direction in a prototype among the Q1D materials, the tetrachalco-halogenide $(\text{TaSe}_4)_2\text{I}$. In this context, earlier experimental studies on the compounds TTF-TCNQ (Ref. 12) and $(\text{SN})_x$ (Ref. 13) suffered in the former to some extent from the effects of twinning and in the latter came to the conclusion that the material studied should not be viewed as a Q1D metal but rather as an anisotropic 2D or 3D conductor, and both materials play no role in view of the current discussion of Q1D conductors. Plasmon excitations have also been studied in other classes of Q1D systems such as the semiconducting polyacetylene¹⁴ or quantum-wire electron systems.¹⁵ However, these systems differ significantly from the conducting Q1D compounds treated here and therefore will not be discussed further. The plasmon dispersion itself is known to be a sensitive probe of the importance of correlation and exchange effects. As these are the fundamental reason for the LL behavior in 1D, the study of the plasmon excitation is specifically suited to our objectives.

II. EXPERIMENTAL

The $(\text{TaSe}_4)_2\text{I}$ single crystals were prepared from the stoichiometric mixture of the elements by evaporation in a closed quartz crucible at temperatures between 480 and 510 °C.¹⁶ Characterization and orientation of the resulting needle-shaped single crystals were carried out by means of x-ray diffraction. For the measurements of the plasmon dispersion using electron energy-loss spectroscopy (EELS) in transmission, free-standing films of about 1000 Å thickness were cut from the crystals using an ultramicrotome equipped

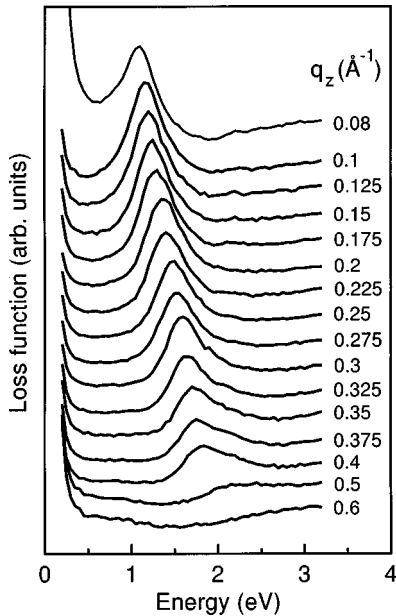


FIG. 1. Normalized electron-energy loss spectra of $(\text{TaSe}_4)_2\text{I}$ for different momentum transfers along the 1D direction.

with a diamond knife. The nearly perfect crystallinity along the 1D direction, which is parallel to the crystallographic c -axis, was proven by *in situ* electron diffraction. The EELS measurements were performed at room temperature using a purpose-built spectrometer¹⁷ with a primary electron energy of 170 keV. The energy and momentum resolution was chosen to be 115 meV and 0.05 \AA^{-1} , respectively.

III. RESULTS AND THEORETICAL INTERPRETATION

In Fig. 1 we show a series of energy-loss spectra recorded for different momentum transfer along the 1D direction. The curves are normalized to a feature observed between about 7 and 8 eV (not shown). For energies less than about 0.5 eV the contribution of the direct beam can be seen, which is broadened due to quasielastic scattering and remains quite strong even at higher momentum transfers because the Ta ions act as strong scattering centers. Clearly separated from this zero loss peak, at least for momentum transfers larger than 0.1 \AA^{-1} , the strongly dispersing plasmon peak related to the oscillations of the free charge carriers is observed. For momentum transfers up to 0.325 \AA^{-1} the width of the plasmon stays nearly constant, but increases sharply at 0.35 \AA^{-1} (see inset to Fig. 2). At still higher momentum transfers, the width increases further until the plasmon vanishes between 0.5 and 0.6 \AA^{-1} . Within the random-phase approximation (RPA), a plasmon in one dimension cannot decay into electron-hole pairs as is normally the case in three dimensions above a critical wave vector (often referred to as Landau damping).¹⁸ Hence the reason for the sudden increase in the width of the plasmon peak lies mainly in the fact that with increasing momentum transfer the plasmon enters the continuum of interband transitions. From optical measurements¹⁹ or tight-binding (TB) band-structure calculations²⁰ this continuum is known to begin slightly below 2 eV. Thus one can speak of a well-defined plasmon excitation up to momentum transfers of about 0.4 \AA^{-1} .

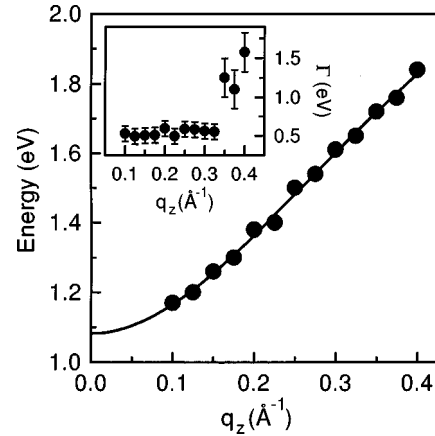


FIG. 2. Experimental (dots) and theoretical (line) plasmon dispersion for $(\text{TaSe}_4)_2\text{I}$. The inset depicts the plasmon width Γ as a function of momentum transfer q_z .

The dispersion relation of the free charge carrier plasmon is plotted in Fig. 2 together with a fit to the data resulting from the theoretical approach described in detail below. The experimental energy positions were determined by simply taking the maximum of a fitted Drude peak. The agreement between the plasmon dispersion from the experiment and from the fit within our model is excellent over the whole range of momentum transfer, which is accessible with our technique and covers the Γ -Z direction of the first Brillouin zone with respect to the bare Ta lattice from about 10 to 40%. At first glance the measured dispersion may be described as quasilinear. The situation encountered in $(\text{TaSe}_4)_2\text{I}$ has been treated quite comprehensively by Williams and Bloch¹⁸ in a more general context. They consider a square array of one-dimensional chains within the RPA in two extreme cases: the limits of free and of tightly bound electrons with a first-nearest-neighbor hopping (within the chains) in one dimension. An inhomogeneous charge distribution along and perpendicular to the chains is taken into account as well as an interchain coupling via the Coulomb interaction. For free electrons they arrive at a q^2 dependence for the plasmon dispersion along the chain direction in the long-wavelength approximation, which would yield a clearly curved shape on the momentum scale of Fig. 2. Assuming a TB model, no parameter independent qualitative behavior can be extracted from their theory. A fit of our data according to their model in this case does not lead to convincing agreement. We note that other models restricted to exactly one dimension suffer from the fact that they cannot account for finite plasmon energy at zero momentum because in one dimension the collective plasmon excitations would be acoustic in nature.²¹

In the following we demonstrate that the observed plasmon dispersion can be understood as resulting purely from the specific band structure of $(\text{TaSe}_4)_2\text{I}$. The result of the TB calculation of Gressier *et al.*²⁰ for a TaSe_4 chain (solid lines) is shown in Fig. 3. The Brillouin-zone boundary at π/c (c is the lattice constant in the chain or z direction, $c = 12.825 \text{ \AA}$) corresponds to the crystallographic unit cell that contains two chains with four Ta ions on each. The Brillouin-zone boundary of the underlying Ta lattice—whose d states form the bands of interest—is $4\pi/c$ ($\equiv G_z/2$, G_z is the component

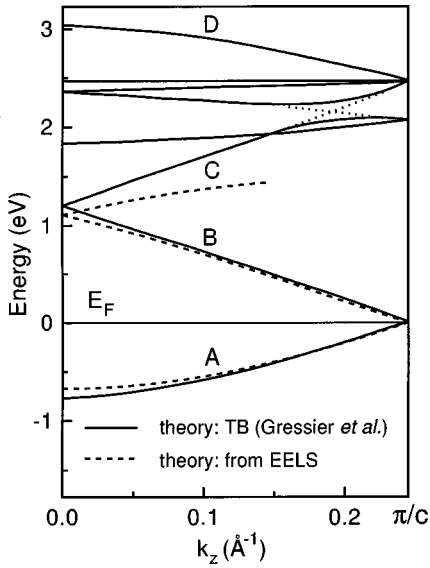


FIG. 3. Comparison of the conduction band of $(\text{TaSe}_4)_2\text{I}$ along the 1D axis as obtained from the theoretical curve shown in Fig. 2 (dashed line) and tight-binding band-structure calculations from Ref. 20 (solid line). The Fermi energies are chosen to coincide for both cases ($E_F=0$ eV). For details see the text.

of the primitive reciprocal lattice vector in the z -direction). Electron counting yields that band A is fully occupied, which is equivalent to a quarter-filling of one d band of the Ta chain. The bands A, B, and D have $d_{3z^2-r^2}$ character throughout the zone. Band C has the same character near the center of the zone but d_{xy} and $d_{x^2-y^2}$ character at the zone boundary because two bands having d_{xy} and $d_{x^2-y^2}$ character overlap with band C (which is made clear by the dotted lines for the noninteracting bands in Fig. 3). The bands A and B are degenerate at the zone boundary, the bands B and C at the zone center. They do not show any tetramerization due to the fact that at the dihedral angle $\Theta=45^\circ$ (between adjacent Se_4 units on the same chain) there is no interaction between the Ta $d_{3z^2-r^2}$ orbital and the Se π and π^* orbitals.

Since the observed plasmon energies (Fig. 2) are less than 1.9 eV, the bands in the energy range up to $E_F+1.9$ eV are of special interest. These are the bands A, B, and the first half of band C. As already mentioned, these all have the same symmetry, which means that normal interband transitions between them are forbidden. Thus, only umklapp interband transitions $A \rightarrow B$ and $A \rightarrow C$ are possible. As the bands A, B, and C have a folded structure, one can represent them in the extended zone scheme of the underlying Ta lattice with the zone boundary at $4\pi/c$. In this representation, the *umklapp interband* transitions $A \rightarrow B$ and $A \rightarrow C$ appear as *normal intraband* transitions. In the following only the intraband transitions for a single 1/4-filled band are considered. This is convenient for the calculations, but not principally necessary.

Since the onset of normal interband transitions is at higher energies (≈ 2 eV) the imaginary part of the dielectric function will be small below this energy and the plasmon excitation is determined by the zero of the real part of the dielectric function:

$$0 = \varepsilon_1(\mathbf{q}, \omega) \approx \varepsilon_s - \frac{4\pi e^2}{q^2} \frac{2}{(2\pi)^3} \int d^3k \frac{2f(E_{\mathbf{k}})\Delta E_{\mathbf{k},\mathbf{q}}}{(\hbar\omega)^2 - (\Delta E_{\mathbf{k},\mathbf{q}})^2}, \quad (1)$$

where f is the Fermi distribution function and $\Delta E_{\mathbf{k},\mathbf{q}} = E_{\mathbf{k}+\mathbf{q}} - E_{\mathbf{k}}$ is the intraband (conduction-band) excitation energy for a momentum transfer \mathbf{q} . In Eq. (1) we use the 3D Ehrenreich-Cohen expression²² for the dielectric function, but take into account the 1D nature of the conduction band. Contributions to the dielectric function from core-level transitions are described by a static dielectric constant ε_s . As explained above, we include in the dielectric function only the normal intraband transitions from band A to the defolded bands B and C. The additional modulation of the electronic density by the lattice, known as crystal local-field effects, are of the order $(2q_z/G_z)^2$. This can be seen from the general expression for the dielectric matrix and from the direct calculations of the matrix elements with the electrons localized to the chains for the TB limit.¹⁸ In our case $(2q_z/G_z)^2$ is 0.01 and 0.16, respectively, for the minimum (0.1 \AA^{-1}) and maximum (0.4 \AA^{-1}) momentum transfer considered here, and therefore the above-mentioned lattice effects are small.²³ The most important lattice effect is the \mathbf{k} dependence of the electron energy $E_{\mathbf{k}}$, which is included in Eq. (1).

The TB parametrization of the $d_{3z^2-r^2}$ band corresponding to the defolded band A to C in the extended zone scheme is

$$E_{k_z} = 2t_1 \left[1 - \cos\left(k_z \frac{c}{4}\right) \right] + 2t_2 \left[1 - \cos\left(k_z \frac{c}{2}\right) \right], \quad (2)$$

where t_1 and t_2 are the hopping integrals between nearest and next-nearest neighbors.

With a least-squares fit using the numerically evaluated $\varepsilon_1(q_z, \omega)$, the theoretical values for the plasmon energy derived from Eq. (1) can be fitted to the experimental data. It should be mentioned that the model contains as fit parameters only the static dielectric constant and the two hopping integrals. Figure 2 shows that the fit (solid line) agrees almost perfectly with the experimental data. It yields a static dielectric constant $\varepsilon_s=10.1$, the hopping integrals $t_1=0.53$ eV and $t_2=0.18$ eV, and for the long-wavelength limit of the plasmon energy $\hbar\omega_p=1.08$ eV. This value is in good agreement with that of about 1.1 eV as obtained from reflectance measurements.²⁴

With the values for the two hopping integrals from our fit, the band defined by Eq. (2) gives, when folded back, the bands shown with dashed lines in Fig. 3. The agreement with the TB calculations of Ref. 20 is surprisingly good for the bands A and B with a maximum deviation of about 10%. The deviation is somewhat larger (up to 25%) for band C up to the wave number $k_z=0.15 \text{ \AA}^{-1}$ corresponding to a momentum transfer of 0.4 \AA^{-1} . Since the orbital character of band C changes at higher k_z this deviation is not unexpected. Additionally, transitions with a large momentum transfer q_z and crystal local-field effects become more important in this region. In general, the method developed here works well in cases where the intraband transitions dominate the plasmon excitations, which applies to $(\text{TaSe}_4)_2\text{I}$ since at first the onset

of normal interband transitions is at high enough energies and, more importantly, due to the low (quarter) filling of the Ta-chain $d_{3z^2-r^2}$ band.

IV. CONCLUSIONS

To summarize, we have carried out a joint experimental and theoretical investigation of the plasmon dispersion in the model Q1D conductor $(\text{TaSe}_4)_2\text{I}$. As in the case of the dc conductivity, a fully satisfying description of the experimental data is obtained in terms of an essentially 3D but strongly anisotropic model. This is in contrast to PES measurements where the absence of a characteristic Fermi cutoff was interpreted as a signal of LL behavior. Indeed, our theoretical approach additionally allows us to derive, besides the static dielectric constant, the dispersion of the band hosting the charge carriers that participate in the plasma oscillations. In this sense a generalization of this combined spectroscopic and theoretical approach represents a new supplementary method for the determination of the bulk electronic band

structure, especially in the case of 1D materials where the well-established methods, such as angle-resolved photoemission and inverse photoemission spectroscopy, may encounter difficulties inherent specifically to these techniques. As already mentioned, the specific 1D LL behavior may still be observable in a certain intermediate regime as the 3D Coulomb interaction is switched on and electron hopping is allowed perpendicular to the chains. Thus, to explain the striking difference to the conclusions drawn from the PES data, we conclude that the effective 3D interaction will alter for different experimental methods depending on the different response functions being probed.

ACKNOWLEDGMENTS

We are grateful to S.-L. Drechsler and R. Claessen for fruitful discussions, and thank M. S. Golden for a critical reading of the manuscript. V.G.G. and G.P. gratefully acknowledge financial support by the Deutsche Forschungsgemeinschaft (DFG).

-
- ¹B. Dardel, D. Malterre, M. Grioni, P. Weibel, Y. Baer, and F. Lévy, *Phys. Rev. Lett.* **67**, 3144 (1991).
- ²C. Coluzza, H. Berger, P. Alméras, F. Gozzo, G. Margaritondo, G. Indelkofer, L. Forro, and Y. Hwu, *Phys. Rev. B* **47**, 6625 (1993).
- ³G.-H. Gweon, J. W. Allen, R. Claessen, J. A. Clack, D. M. Poirier, P. J. Benning, C. G. Olson, W. P. Ellis, Y.-X. Zhang, L. F. Schneemeyer, J. Marcus, and C. Schlenker, *J. Phys.: Condens. Matter* **96**, 9923 (1996).
- ⁴C. Schlenker and J. Dumas, in *Crystal Chemistry and Properties of Materials with Quasi-One-Dimensional Structures*, edited by J. Rouxel (Reidel, Dordrecht, 1986), p. 135.
- ⁵Z. Z. Wang, M. C. Saint-Lager, P. Monceau, M. Renard, P. Gressier, A. Meerschaut, L. Guemas, and J. Rouxel, *Solid State Commun.* **46**, 325 (1983).
- ⁶For a review see J. Voit, *Rep. Prog. Phys.* **57**, 977 (1994).
- ⁷J. Voit, *Phys. Rev. B* **47**, 6740 (1993).
- ⁸K. Schönhammer and V. Meden, *Phys. Rev. B* **47**, 16 205 (1993).
- ⁹P. Kopietz, V. Meden, and K. Schönhammer, *Phys. Rev. Lett.* **74**, 2997 (1995).
- ¹⁰W. Brütting, P. H. Nguyen, W. Rieß, and G. Paasch, *Phys. Rev. B* **51**, 9533 (1995).
- ¹¹W. Brütting, W. Rieß, P. H. Nguyen, and G. Paasch, in *The Physics of Semiconductors*, edited by M. Scheffler and R. Zimmernann (World Scientific, Singapore, 1996), Vol. 4, p. 3363.
- ¹²J. J. Ritsko, D. J. Sandman, A. J. Epstein, P. C. Gibbons, S. E. Schnatterly, and J. Fields, *Phys. Rev. Lett.* **34**, 1330 (1975).
- ¹³C. H. Chen, J. Silcox, A. F. Garito, A. J. Heeger, and A. G. MacDiarmid, *Phys. Rev. Lett.* **36**, 525 (1976).
- ¹⁴J. Fink and G. Leising, *Phys. Rev. B* **34**, 5320 (1986).
- ¹⁵S. Das Sarma and E. H. Hwang, *Phys. Rev. B* **54**, 1936 (1996), and references therein.
- ¹⁶P. Gressier, L. Guemas, and A. Meerschaut, *Acta Crystallogr., Sect. B: Struct. Crystallogr. Cryst. Chem.* **38**, 2877 (1982).
- ¹⁷J. Fink, *Adv. Electron. Electron Phys.* **75**, 121 (1989).
- ¹⁸P. F. Williams and A. N. Bloch, *Phys. Rev. B* **10**, 1097 (1974).
- ¹⁹D. Berner, G. Scheiber, A. Gaymann, H. P. Geserich, P. Monceau, and F. Lévy, *J. Phys. IV* **3**, C2-255 (1993).
- ²⁰P. Gressier, M.-H. Whangbo, A. Meerschaut, and J. Rouxel, *Inorg. Chem.* **23**, 1221 (1984).
- ²¹S. Das Sarma and W. Y. Lai, *Phys. Rev. B* **32**, 1401 (1985).
- ²²H. Ehrenreich and M. H. Cohen, *Phys. Rev.* **115**, 786 (1959).
- ²³We note that for the model of free electrons in 1D and $\mathbf{q} = (0, 0, q_z)$ the matrix element is equal to one, and Eq. (1) holds exactly. See also Ref. 18.
- ²⁴H. P. Geserich, G. Scheiber, F. Lévy, P. Gressier, and P. Monceau, *Mol. Cryst. Liq. Cryst.* **121**, 19 (1985).